Small Colonic Microsatellite Unstable Adenocarcinomas and High-Grade Epithelial Dysplasias in Sessile Serrated Adenoma Polypectomy Specimens

A Study of Eight Cases

Neal S. Goldstein, MD

Key Words: Serrated adenoma; Sessile; Colon; Polyp; Microsatellite instability

DOI: 10.1309/V8Q9KDD5AJ9LNBAG

Abstract

Eight sessile serrated adenoma (SSA), right colon polypectomies with focal invasive adenocarcinoma or high-grade dysplasia were studied to identify features indicating a high risk of transformation and characterize the morphologic features of serrated dysplasia; 6 cases had invasive adenocarcinoma; 2 were high-grade dysplasia. All 8 were microsatellite unstable-high and had absent hMLH1 nuclear immunoreactivity. The mean patient age at polypectomy was 69.5 years (range, 57.1-83.9 years). Mean polyp maximum dimension was 8.5 mm (range, 6-12 mm). The majority of each polyp was nonmalignant SSA. All 8 cases had an abrupt transition from benign to high-grade in situ or invasive malignancy. In the 6 invasive adenocarcinomas, the neoplasm extended directly down into the submucosa without lateral intramucosal spread. The mean maximum dimension of the invasive adenocarcinoma was 2.9 mm (range, 2-4 mm). All 8 cases had high-grade serrated-type dysplasia. The nonmalignant SSAs had marked expansion of the proliferative zone. Crypts adjacent to malignancy had moderately enlarged nuclei, irregular nuclear membranes, and overly prominent nucleoli. SSA crypts were lined by a variety of gastric-type cells; no cell type predominated. Foci of adjacent crypts had similar cytologic features. Small proximal SSAs can transform into adenocarcinoma without a component of adenomatous dysplasia.

The serrated neoplasia pathway has its underpinnings in a recently characterized molecular mechanism that eventuates in microsatellite unstable-high (MSI-high) colorectal adenocarcinomas. Kambara et al[1] suggested that some serrated polyps were the precursors in this pathway. Early and late serrated neoplasia pathway lesions have been the focus of studies, and knowledge about these lesions has started to accrue. Midpathway lesions with noninvasive malignancy or small volumes of invasive adenocarcinoma are rare lesions and have not been studied thoroughly. These lesions may provide insight into several current issues that are the subject of active debate. It has been suggested that transformation from serrated pathway precursor to invasive adenocarcinoma can be rapid and occur when the lesions are small; however, evidence supporting these events is scant.[2-4] Morphologic features that portend an increased risk of neoplastic transformation are unknown. This study evaluated 8 serrated neoplasia pathway polyps with incidental high-grade dysplasia or invasive adenocarcinoma to address these issues.

Materials and Methods

Study Cases

Permission for the study was granted by the William Beaumont Hospital (Royal Oak, MI) Human Investigations Committee (HIC No. E2005-022). An initial search of the William Beaumont Hospital anatomic pathology computer was performed for American Joint Committee on Cancer stage 1, Tis, or T1 colorectal adenocarcinoma cases from patients who were at least 60 years old in whom the malignancy was

found in an endoscopically resected polypectomy specimen and who underwent subsequent regional colectomy during the period January 1, 1985, through January 10, 2005. A cut point of at least 60 years old was included as a search parameter to negate the likelihood that a study group patient had hereditary nonpolyposis colorectal cancer syndrome–related malignancy and to increase the proportion of microsatellite unstable adenocarcinomas in the initial pool of neoplasms.

Slides and surgical pathology reports were reviewed. Cases were excluded if the polyp was resected in small fragments using a biopsy forceps cup rather than a snare electrothermal loop; the lesion was an unequivocal, nonserrated, conventional, low-grade tubular, tubulovillous, or villous adenoma; or the polypectomy specimen did not contain high-grade epithelial dysplasia or invasive adenocarcinoma. Cases also were excluded if the majority of the polypectomy specimen was composed of malignant epithelium (polypoid adenocarcinoma) or if the invasive adenocarcinoma was a nonpolypoid flat or depressed lesion that extended into the deep submucosa.

Specimen blocks were obtained from storage and examined to confirm there was adequate residual tissue. The color of the paraffin in each block was confirmed to be white or translucent, indicating the tissue had been fixed in formalin and was suitable for immunohistochemical and molecular studies. Cases in which the paraffin in the blocks was yellow or gray, indicating the tissue had been fixed in Bouin or B-5 fixative, were excluded. Four serial sections were first cut from the suitable blocks for hMLH1 immunohistochemical analysis (see the "Immunohistochemical Analysis" section) followed by careful microdissection of the malignant lesion for microsatellite instability analysis (see the "Microsatellite Instability" section). Cases with insufficient residual tissue in the paraffin blocks to perform both studies were excluded. Cases also were excluded if the invasive adenocarcinoma or high-grade epithelial dysplasia had hMLH1 nuclear immunoreactivity or if they were microsatellite stable or microsatellite unstable-low (MSI-low).

Following these exclusionary procedures, 8 serrated polyps with invasive adenocarcinoma or high-grade epithelial dysplasia had absent hMLH1 nuclear immunoreactivity and were MSI-high, the defining molecular signature of serrated neoplasia pathway malignancy. These 8 cases constituted the study lesions. All 8 were endoscopically resected, snare-polypectomy specimens composed predominantly of nonmalignant serrated polyp with a small focus of invasive adenocarcinoma or high-grade epithelial dysplasia. All 8 study patients underwent colonoscopy as a repeated surveillance procedure owing to previous colonic adenomas or as an initial screening procedure. None had signs or symptoms suggesting the presence of an adenocarcinoma.

Control group cases were tubular and tubulovillous adenomas obtained from 10 conventional familial adenomatous polyposis (FAP) syndrome complete proctocolectomy resection specimens. Gene sequencing mutation confirmed the classic form of FAP in all 10 specimens. All 10 specimens were blanketed diffusely by "thousands" of mucosal polyps of varying sizes. Three specimens also had one to several large polypoid, fixed masses. Three slides from 3 separate, large (>2 cm), freely mobile mucosal polyps were selected randomly from each case, resulting in 30 control cases of conventional tubular or tubulovillous adenoma. These cases were used to establish and benchmark the cytologic features of adenomatous dysplasia. Adenomas from patients with FAP were used to avoid bias regarding the definition of conventional adenoma.[5]

Pathologic Features and Definitions

The following factors were recorded in each study case:

1. Number of polypectomy tissue blocks.
2. Maximum polyp dimension, measured on the glass slide.
3. Maximum dimension of invasive adenocarcinoma or high-grade dysplasia, measured on the glass slide.
4. Adenocarcinoma mucosal invasion location, classified as superficial crypt region, mid crypt region, or basilar crypt region.
5. Invasive adenocarcinoma cytologic features and the proportion of each distinct subtype (if multiple), classified as columnar not otherwise specified (NOS) or cuboidal-eosinophilic: *columnar NOS invasive adenocarcinoma,* pseudostratified columnar cells with hyperchromatic chromatin, variable sized nucleoli, and scant to moderate amounts of amphophilic to eosinophilic cytoplasm; *cuboidal-eosinophilic invasive adenocarcinoma,* cuboidal to blunted short columnar cells with round to oval nuclei, open chromatin, prominent nucleoli, and dense eosinophilic cytoplasm.
6. High-grade epithelial dysplasia location within mucosa (if present), classified as superficial crypt region, mid crypt region, or basilar crypt region. High-grade epithelial dysplasia was defined as noninvasive epithelial cells with frankly malignant cytologic features.
7. Cytologic features of high-grade dysplasia epithelial cells and the proportion of each distinct subtype (if multiple), classified as adenomatous polyposis coli (APC) type, serrated type, or high-grade NOS: *APC-type epithelial dysplasia* had the cytologic features of conventional tubular or tubulovillous adenomas from control group patients (FAP syndrome) **Image 1**. Cells had a narrow range of cytologic alterations. They were uniformly thin and columnar shaped with pseudostratified, pencillate nuclei. Nuclear membranes were fairly smooth with an incomplete, longitudinally oriented groove. Chromatin was uniformly hyperchromatic and coarse. No nucleolus could be seen

DOI: 10.1309/V8Q9KDD5AJ9LNBAG

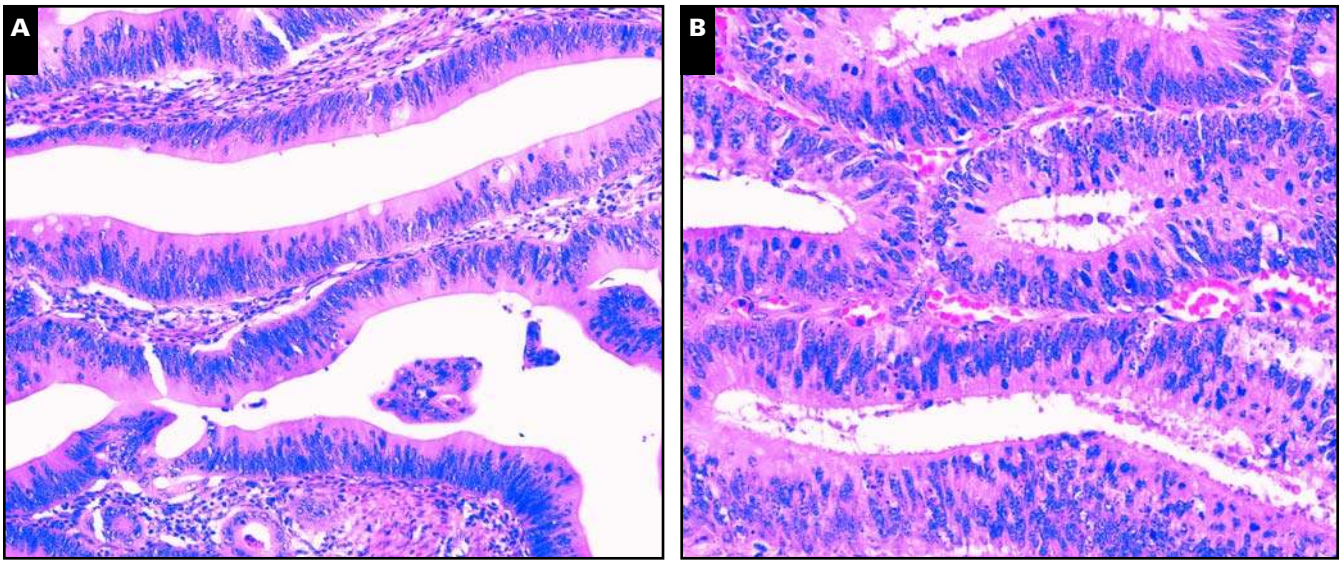

Image 1 Adenomatous polyposis coli (APC)-type dysplasia, familial adenomatous polyposis control group tubular adenoma. The cytologic features are monomorphous. The neoplastic cells are uniformly thin and columnar with pseudostratified, pencillate nuclei. The chromatin pattern is uniform and coarse. Nucleoli are punctate. Most cells have homogeneous eosinophilic cytoplasm. **A**, Low-grade APC-type dysplasia (H&E, ×120). **B**, High-grade APC-type dysplasia. Nuclear alterations are extreme, yet they retain sufficient characteristic features to be recognized as APC-type dysplasia (H&E, ×240).

in approximately half the cells; the remainder of the cells had 1 or 2 punctate nucleoli. Most cells had homogeneous eosinophilic cytoplasm. Insolated, well-developed goblet mucus cells were interspersed. High-grade APC-type dysplasia consisted of marked cytologic and nuclear alterations including larger and occasionally more oval nuclei, greater nuclear size variation, and marked nuclear membrane irregularities including notches, infoldings, and grooves. The chromatin had a uniformly coarse background pattern. In addition, numerous dark chromatin dots were situated adjacent to or appeared attached to the inner nuclear membrane. A large minority of the cells had small apical cytoplasmic mucin pools. Goblet cells were decreased compared with low-grade APC-type dysplasia. Despite the more extreme cytologic alterations, the cells of high-grade APC-type dysplasia remained markedly monomorphic and retained their thin shape, picket fence-like arrangement, and cigar-shaped nuclei. Retention of these cytologic features often continued in the cells of the associated invasive adenocarcinomas (not shown).

Serrated-type epithelial dysplasia, cuboidal to short columnar cells with basilar, round to oval nuclei, open chromatin, a prominent macronucleolus, and a minimal to moderate amount of cytoplasm **Image 2**, **Image 3**, **Image 4**, and **Image 5**. High-grade, serrated-type dysplasia consisted of cuboidal-eosinophilic dysplastic cells with substantially larger nuclei, irregular thickenings of the nuclear membrane, and a dense dark macronucleolus.

High-grade, NOS epithelial dysplasia, undifferentiated, extremely high-grade malignant cells devoid of characteristic cytologic features of either form of cytologic dysplasia (Image 4) **Image 6** and **Image 7**.

8. Proportion of dysmaturational crypts in nonmalignant serrated polyp with differentiation toward distinctive cell types, classified as goblet mucus cell, gastric foveolar mucin cell, eosinophilic enteric cell, or microvesicular columnar.
9. Microsatellite instability status, evaluated in malignant epithelium and nonmalignant serrated epithelium
10. Status of *APC* gene mutation or inactivation in adenomatous epithelium, high-grade dysplasia, or invasive adenocarcinoma. Loss of heterozygosity (LOH) of the D5s346 microsatellite marker, located adjacent to the *APC* gene, within the deleted *APC* gene region was recorded in informative cases (2 distinct allelic peaks). LOH was defined as allelic loss of ±50% of the normal tissue allelic ratio.[6] β-catenin immunoreactivity was assessed. A normal staining pattern had strong membranous, weak cytoplasmic, and absent nuclear β-catenin immunoreactivity. Adenomas and adenocarcinomas from patients with FAP had weak or absent membranous, weak cytoplasmic, and strong nuclear β-catenin immunoreactivity. *APC* was considered mutated if adenocarcinoma cells showed

DOI: 10.1309/V8Q9KDD5AJ9LNBAG

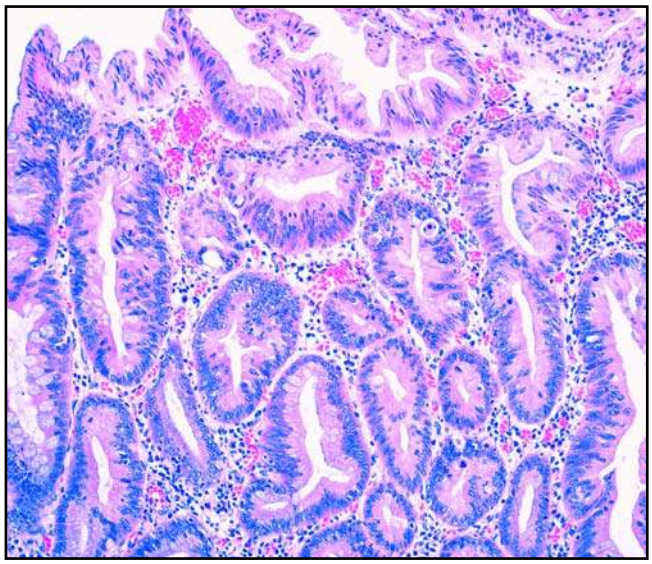

Image 2 (Case 1) High-grade serrated dysplasia in crypts overlying invasive adenocarcinoma in the left and right portions of the image. Crypts in middle of the image have cytologic alterations slightly less than high-grade dysplasia. Cells throughout the image have basilar cuboidal nuclei with open chromatin. Their cytoplasm shows abortive gastric foveolar columnar mucin cell differentiation. Maturational changes are superimposed on high-grade dysplasia (H&E, ×64).

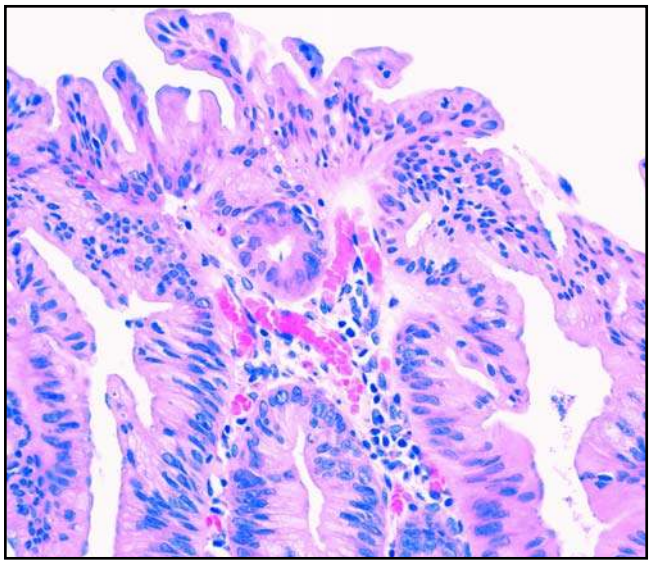

Image 3 (Case 1) Surface region over high-grade serrated dysplasia. The surface cells are lower grade than the subjacent high-grade cells owing to maturational changes. Although atypical, these surface cells are less than high-grade dysplasia. They have smaller nuclei and greater amounts of cytoplasm than the high-grade dysplastic cells in the deeper crypt regions (H&E, ×128).

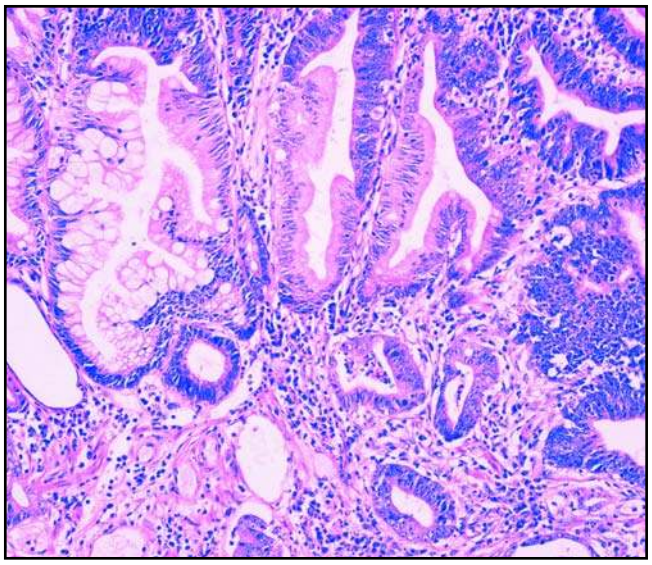

Image 4 (Case 2) Invasive adenocarcinoma glands drop off the bottom of crypts involved by high-grade serrated dysplasia into the submucosa. There is no lateral, intramucosal extension. Despite the basophilic appearance of the high-grade serrated dysplastic cells in the right half of the image, they have round nuclei and prominent nucleoli typical of serrated dysplasia. Crypts in the left portion are lined by eosinophilic cells. One crypt to the left of center has hypermucinous columnar mucin cells. Cells in crypts to the right of center show columnar foveolar mucin cell differentiation (H&E, ×64).

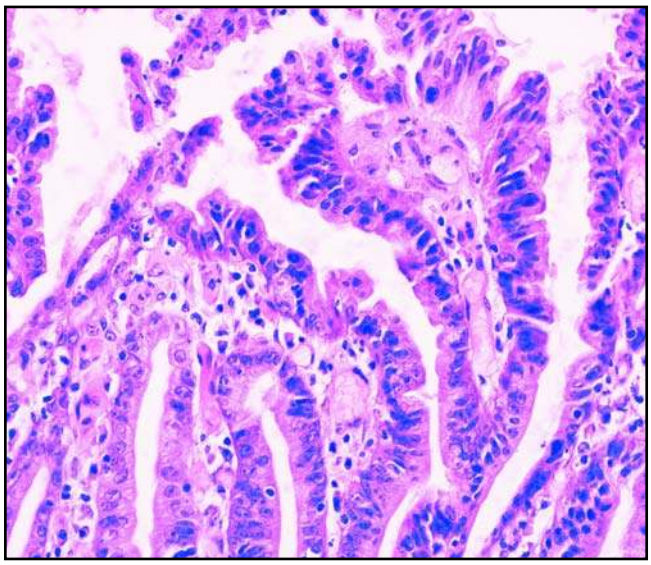

Image 5 (Case 2) Surface of high-grade serrated dysplasia over the invasive adenocarcinoma. Cells are cuboidal to short columnar and have overly large nuclei with open chromatin and prominent nucleoli. The cells in the most superficial crypt region show slight maturational changes with increased cytoplasm and smaller nuclei (H&E, ×256).

DOI: 10.1309/V8Q9KDD5AJ9LNBAG

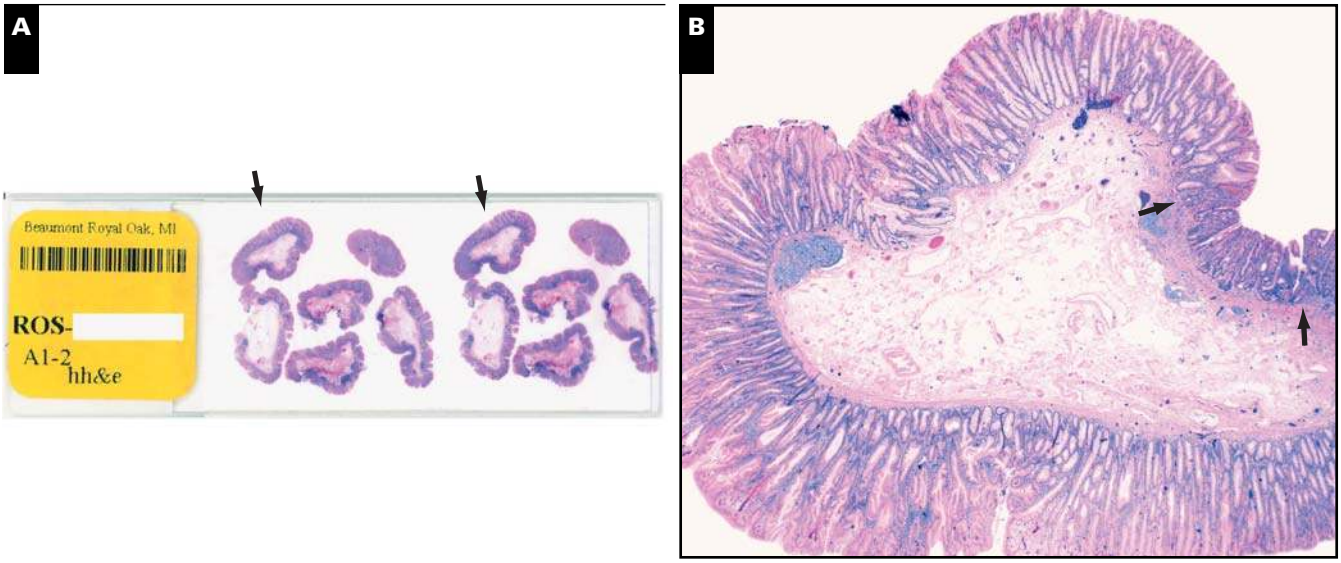

Image 6 (Case 7) **A**, Polyp slide whole-mount image. One section of polyp has a small area of high-grade epithelial dysplasia (arrows). **B**, Microscopic panorama of abrupt transition from sessile serrated adenoma to high-grade epithelial dysplasia, not otherwise specified (H&E, ×8). The 2 arrows bracket the area of high-grade dysplasia.

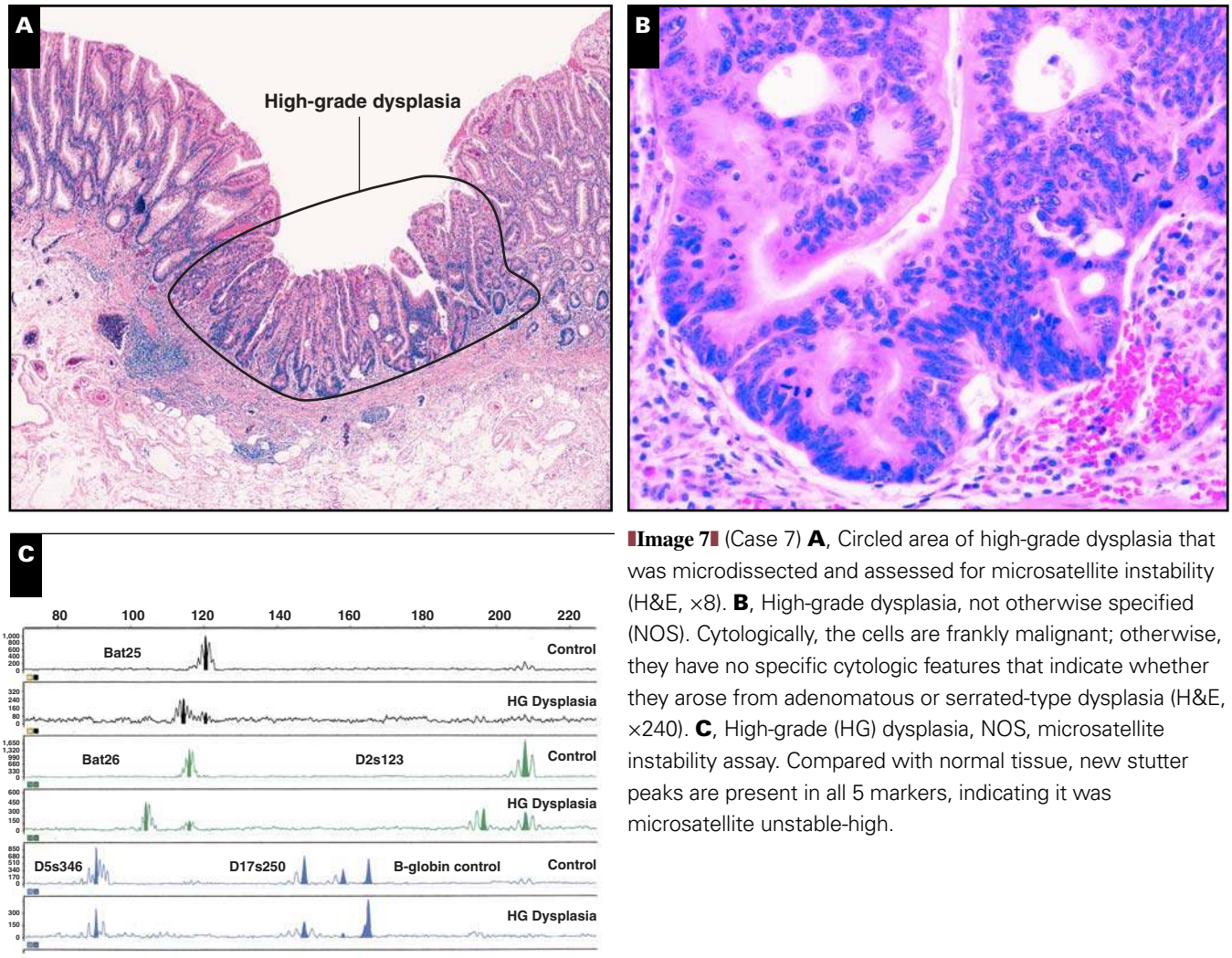

Image 7 (Case 7) **A**, Circled area of high-grade dysplasia that was microdissected and assessed for microsatellite instability (H&E, ×8). **B**, High-grade dysplasia, not otherwise specified (NOS). Cytologically, the cells are frankly malignant; otherwise, they have no specific cytologic features that indicate whether they arose from adenomatous or serrated-type dysplasia (H&E, ×240). **C**, High-grade (HG) dysplasia, NOS, microsatellite instability assay. Compared with normal tissue, new stutter peaks are present in all 5 markers, indicating it was microsatellite unstable-high.

DOI: 10.1309/V8Q9KDD5AJ9LNBAG

decreased membrane and strong nuclear β-catenin immunoreactivity.[7]

11. Previous colonoscopy lesions at the site of the index polypectomy.
12. Serrated dysplasia grade using the criteria of Lazarus et al.[4] These authors divided serrated dysplasia into 3 grades, mild, moderate, and severe. To bring this system in line with current nomenclature conventions, I classified their mild and moderate serrated dysplasia as low-grade and their severe dysplasia as high-grade serrated dysplasia.

Immunohistochemical Analysis

Antibodies used in the study were hMLH1 (clone G168-728, dilution 1:250; Pharmingen, San Diego, CA) and β-catenin (C-terminus, clone CAT-5H10, dilution 1:400; Zymed, San Francisco, CA). Four-micrometer tissue sections were applied to charged slides and dried for 45 minutes in a 60°C oven. Slides were immersed in 1 mmol/L of EDTA buffer solution (pH 8) and placed in an electric pressure cooker (Biocare, Walnut Creek, CA) for 3.5 minutes. The primary antibodies then were incubated over the slides for 30 minutes using an autostainer (DAKO, Carpinteria, CA). Following a series of washes, slides were stained with components of the EnVision+ detection system (DAKO), followed by diaminobenzidine, and a light hematoxylin counterstain.

Microsatellite Instability

Microsatellite instability was evaluated in the neoplastic region of all 8 cases. Adjacent noninvasive epithelium and SSA also was evaluated if sufficient target tissue was retrievable from the paraffin tissue blocks. Each focus of targeted tissue was carefully circled on the glass slide, microdissected out of the tissue block under a dissecting microscope using the slide as a template, and immediately placed in clean, 1.5-mL xylene-filled Eppendorf tubes. Tissue was hydrated through graded alcohols to water.

DNA was extracted from the paraffin using the Qiagen mini paraffin extraction kit (catalog No. 51302, Qiagen, Valencia, CA). The 5 National Cancer Institute consensus microsatellite primers were prepared and labeled with fluorescent dyes from Applied Biosystems, Foster City, CA.[8] For each microsatellite primer, a 10-μL master mix (2.0 μL 10× polymerase chain reaction buffer [Applied Biosystems], 1.6 μL of 25-mmol/L magnesium chloride, 1.6 μL of 2.5-mmol/L deoxynucleoside triphosphates, 0.2 μL of 5U/μL-*Taq,* and 4.6 μL of sterile water), 5 μL of primer mix, and 5 μL of specimen DNA were mixed and loaded onto a preheated thermal cycler for one 5-minute cycle at 95°C, 40 cycles of 95°C for 1 minute, and then 52°C (D17s250) or 58°C (Bat25, D2s123, Bat26, D5s346) for 1 minute, a 2-minute cycle at 72°C, and a 15-minute cycle at 72°C. Products were maintained at 4°C until they were analyzed on an Applied Biosystems 310 capillary electrophoresis genetic analyzer (Applied Biosystems).

For each microsatellite marker, the lesional electrophoresis tracing was compared with the patient's matched normal tissue tracing. An abnormal electrophoresis peak pattern was considered present if there was a shift in the allelic peak of 3 base pairs or more from the most prominent normal tissue allele peak or if the lesional tracing had new, well-defined, thin peaks adjacent to the normal tissue allelic peak.[9-11] Lesions were classified as MSI-low if stutter or additional peaks were present in 1 microsatellite primer and MSI-high if these changes were present in 2 or more microsatellites. All positive results were replicated, and only those with reproducible aberrant results were considered valid. Samples were appropriately diluted or concentrated to optimize the signal peak height to 300 to 2,000 relative fluorescence units.

Results

The mean and median patient ages at index colonoscopy were 69.5 and 69.2 years, respectively (range, 57.1-83.9 years). Five polyps were located in the proximal right colon and 3 in the mid or distal right colon. The mean and median maximum polyp dimensions were 8.3 and 7.5 mm, respectively (range, 6-12 mm) **Table 1**.

Invasive Adenocarcinoma

Six cases (cases 1-6) had invasive adenocarcinoma. The mean and median invasive adenocarcinoma maximum dimensions were 2.8 and 3 mm, respectively (range, 2-4 mm; Table 1). Images of case 1, a sessile serrated adenoma (SSA) with focal invasive adenocarcinoma are shown in **Image 8**, **Image 9**, **Image 10**, **Image 11**, **Image 12**, **Image 13**, **Image 14**, **Image 15**, **Image 16**, and **Image 17** (Images 2 and 3). Images of case 7, with only high-grade, serrated-type dysplasia, are shown in **Image 18** (Images 6 and 7), and images of case 2, an SSA with invasive adenocarcinoma, are shown in **Image 19** and **Image 20** (Images 4 and 5).

Table 1
Maximum Dimension of Serrated Polyps and Malignant Components*

Case No.	Serrated Polyp	Invasive Adenocarcinoma	High-Grade Dysplasia
1	10	3	—
2	6	2	—
3	7	3	—
4	7	2	—
5	8	4	—
6	7	3	—
7	9	—	3
8	12	—	4

* Slide-based measurement in millimeters.

DOI: 10.1309/V8Q9KDD5AJ9LNBAG

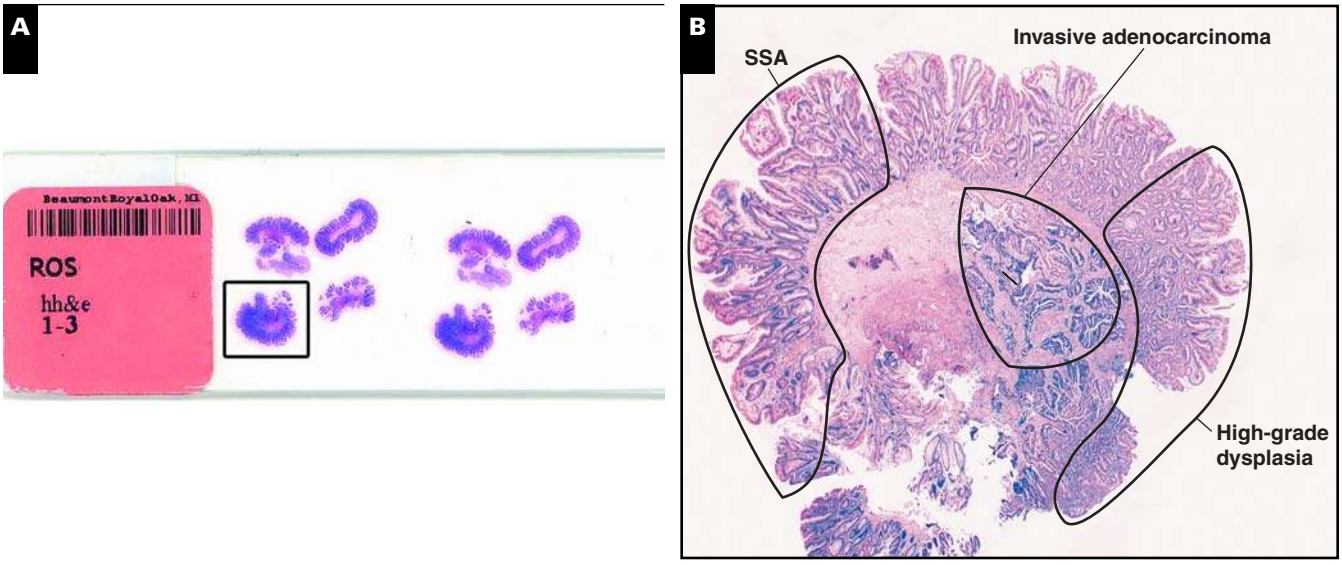

Image 8 (Case 1) **A**, Polyp slide. Section in box was only section with invasive adenocarcinoma. **B**, Microscopic panorama of sessile serrated adenoma (SSA), invasive adenocarcinoma, and overlying high-grade epithelial dysplasia. Circled areas were microdissected and assessed for microsatellite instability (H&E, ×8).

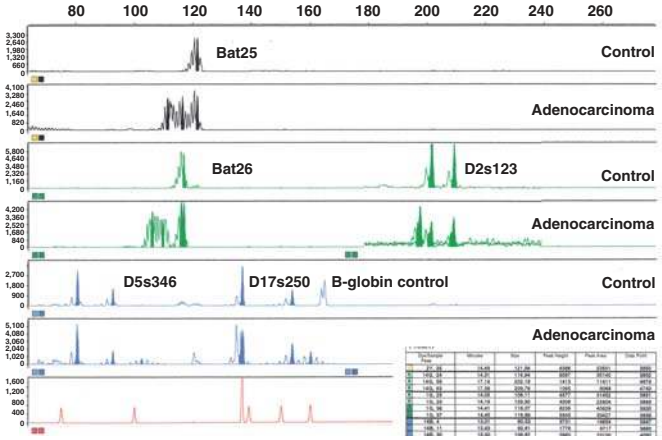

Image 9 (Case 1) Invasive adenocarcinoma, microsatellite instability assay. Compared with normal tissue, new stutter peaks are present in the invasive adenocarcinoma in all 5 markers, indicating it was microsatellite unstable-high. The D2s123 result initially was printed on a separate sheet and was pasted into image to save space.

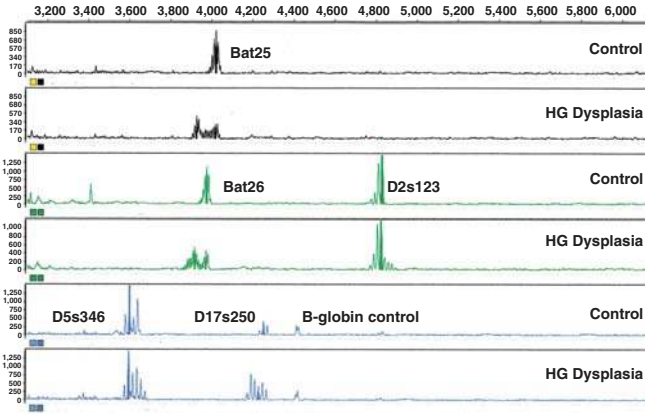

Image 10 (Case 1) High-grade (HG) dysplasia, microsatellite instability assay. Compared with normal tissue, new stutter peaks are present in the high-grade dysplasia in all 5 markers, indicating it was microsatellite unstable-high. The peaks patterns in the high-grade dysplasia differ from the pattern in the invasive adenocarcinoma.

The invasive adenocarcinoma emerged directly from the crypt bases of the overlying mucosa and extended into the submucosa (Images 4 and 11). In some areas, the malignant glands seemed to drop off from noninvasive crypt bases, whereas in other areas, there was intramucosal invasive adenocarcinoma. The invasive adenocarcinoma was similar cytologically to the high-grade epithelial dysplasia in the overlying mucosa. Foci of cuboidal-eosinophilic type adenocarcinoma were present in all cases, which merged into high-grade, NOS-type dysplasia in the submucosa.

The invasive adenocarcinoma extended to the cauterized stalk base in 2 cases and was within the 2-mm rim of cauterized epithelium adjacent to the margin in the other 4 cases. All 6 patients with invasive adenocarcinoma underwent right hemicolectomy or extended colectomy. The polyp attachment site was identified in all 6 colectomy specimens. The mean number of pericolonic lymph nodes examined from the 6 colectomy specimens was 34.6 (range, 15-74). All 6 colectomy specimens were devoid of residual index invasive adenocarcinoma around the site of the granulation tissue

DOI: 10.1309/V8Q9KDD5AJ9LNBAG

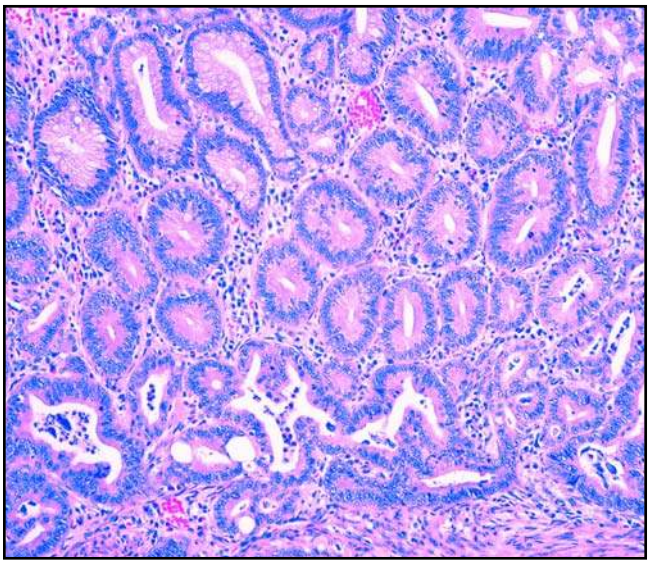

Image 11 (Case1) Invasive adenocarcinoma arises from crypt bases. High-grade, serrated dysplasia is present to the immediate left of the epithelium. The crypts overlying the invasive focus are monomorphic. There is some cytologic similarity to adenomatous polyposis coli-type dysplasia owing to the mucin depletion and basophilic hue (H&E, ×64).

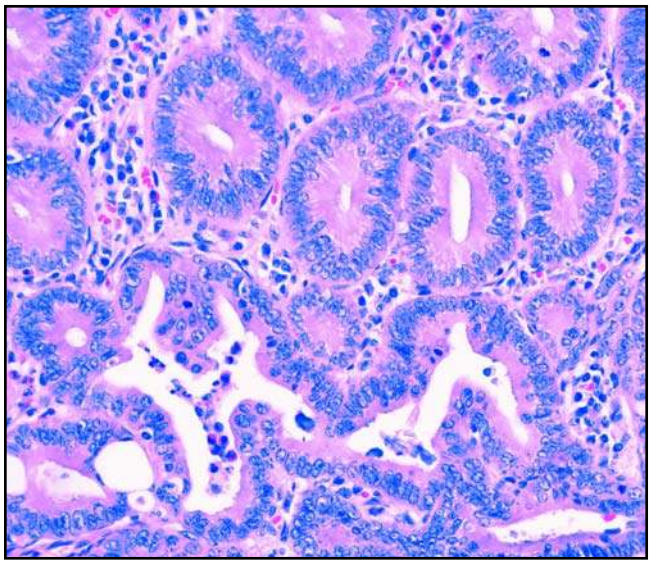

Image 12 (Case 1) Invasive adenocarcinoma, high magnification of Image 11. There is cytologic similarity between the invasive adenocarcinoma and overlying crypts. These crypts have uniform basilar cuboidal nuclei with clear cytoplasm that differs from the features of adenomatous dysplasia in Image 1 (H&E, ×128).

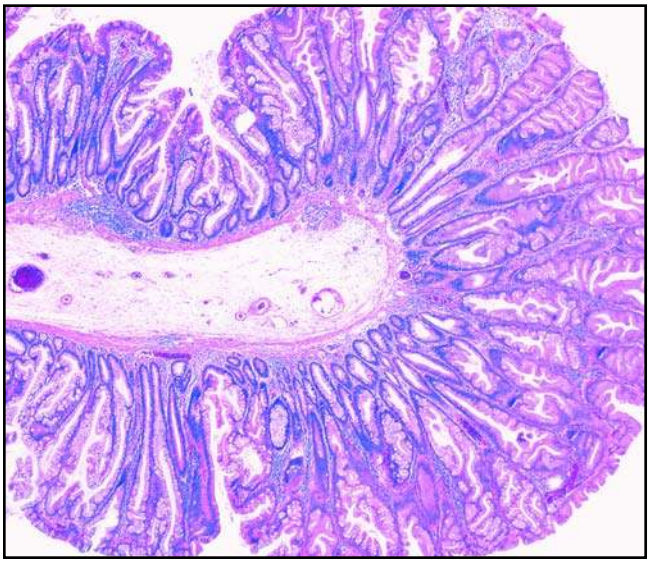

Image 13 (Case 1) Adjacent sessile serrated adenoma. This polyp section is diagonal to the boxed section in Image 8A, whole-slide image (H&E, ×16).

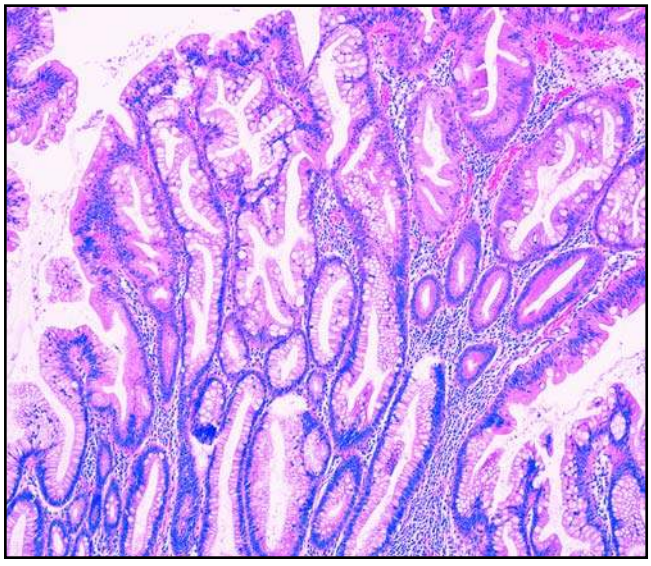

Image 14 (Case 1) Adjacent sessile serrated adenoma, higher magnification of Image 13. Clusters of several adjacent crypts have a similar type of cytoplasmic differentiation. Crypts in the central third of the image have gastric columnar foveolar mucin cell differentiation (H&E, ×32).

attachment site, and all lymph nodes were free of metastatic adenocarcinoma.

High-Grade Epithelial Dysplasia

High-grade epithelial dysplasia was present in all 8 cases. Rather than a field effect process, a single or several adjacent crypts were lined by high-grade dysplastic cells leaving the adjacent crypt uninvolved. A sharp transition from nonmalignant to malignant crypt was present in all 8 cases. In some areas, stellate, irregularly shaped, closely situated clusters of nonserrated tubules were present at the mid crypt level of the lamina propria. In other areas, high-grade dysplastic epithelial cells were located

DOI: 10.1309/V8Q9KDD5AJ9LNBAG

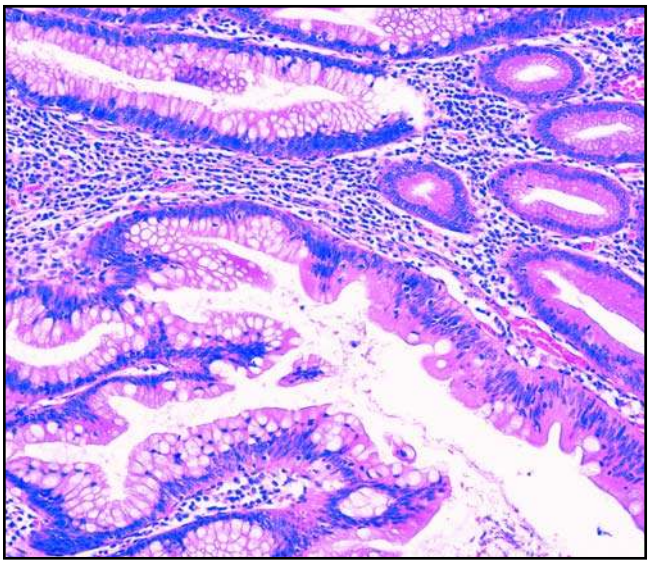

Image 15 (Case 1) Sessile serrated adenoma, higher magnification of Image 14. Lumen is toward the right. There is an abrupt change in cytoplasmic differentiation of cells from gastric foveolar mucin cells in the lower crypt region to eosinophilic nonmucinous in the mid crypt. These cells do not have the features of high-grade dysplasia (H&E, ×64).

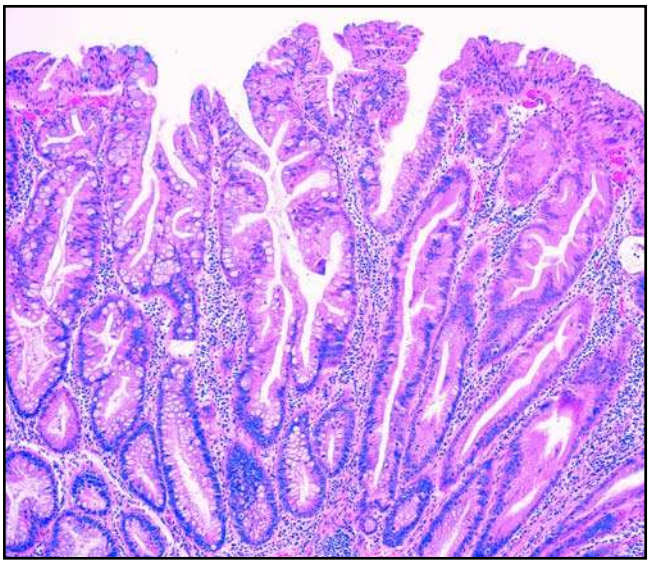

Image 16 (Case 1) Sessile serrated adenoma, higher magnification of Image 14. Four crypts immediately to the right of the midline and in the left half of image have similar cytologic features (H&E, ×64).

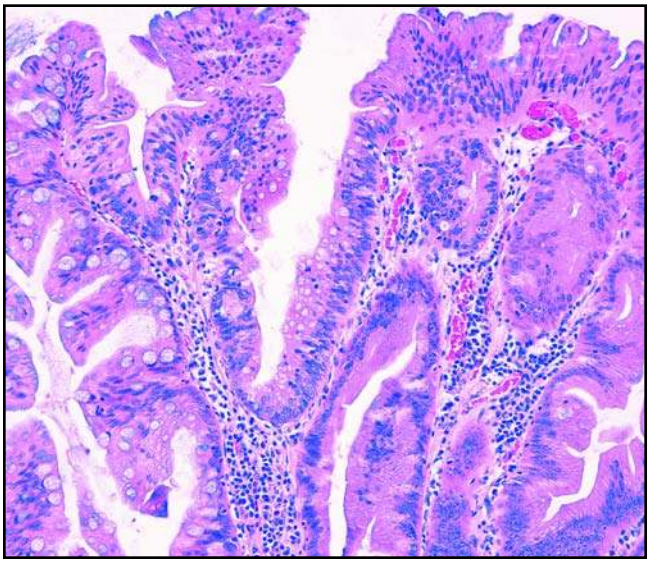

Image 17 (Case 1) Sessile serrated adenoma, high magnification of Image 16. Marked dysmaturational changes extend into the superficial crypt region. Cells of adjacent crypts have variable cytologic differentiation features. The surface epithelium is pseudostratified but otherwise shares no features with adenomatous dysplasia (H&E, ×128).

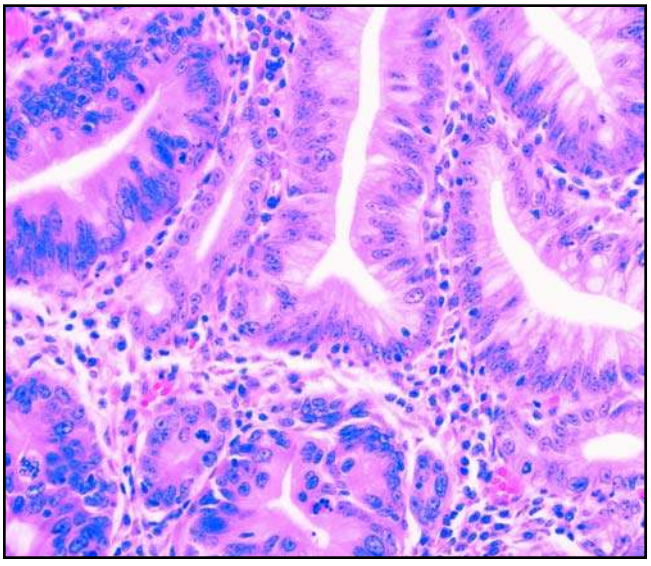

Image 18 (Case 7) Two adjacent crypts, each lined by cells that differ in their grade of dysplasia. High-grade serrated dysplasia is present in the left portion of image. The cells in the right portion of the image have low-grade serrated dysplasia. In the latter areas, the cells are monotonous, and dysmaturational changes are prominent, with immature cells extending into the superficial crypt regions (H&E, ×256).

in the basilar regions of crypts. Similar to adjacent, nonmalignant dysmaturational crypts, high-grade, serrated-type dysplastic epithelial cells displayed cytologic maturation as the cells extended from crypt bases toward the surface. These 2 features produced a bottom-to-top dysplastic-appearing process.

The cytologic features of the high-grade dysplasias are listed in **Table 2**. Serrated-type dysplastic epithelial cells were admixed with high-grade, NOS-type dysplastic cells in 5 cases. One case had only serrated-type epithelial dysplasia, and 2 cases were composed of only high-grade, NOS-type

DOI: 10.1309/V8Q9KDD5AJ9LNBAG

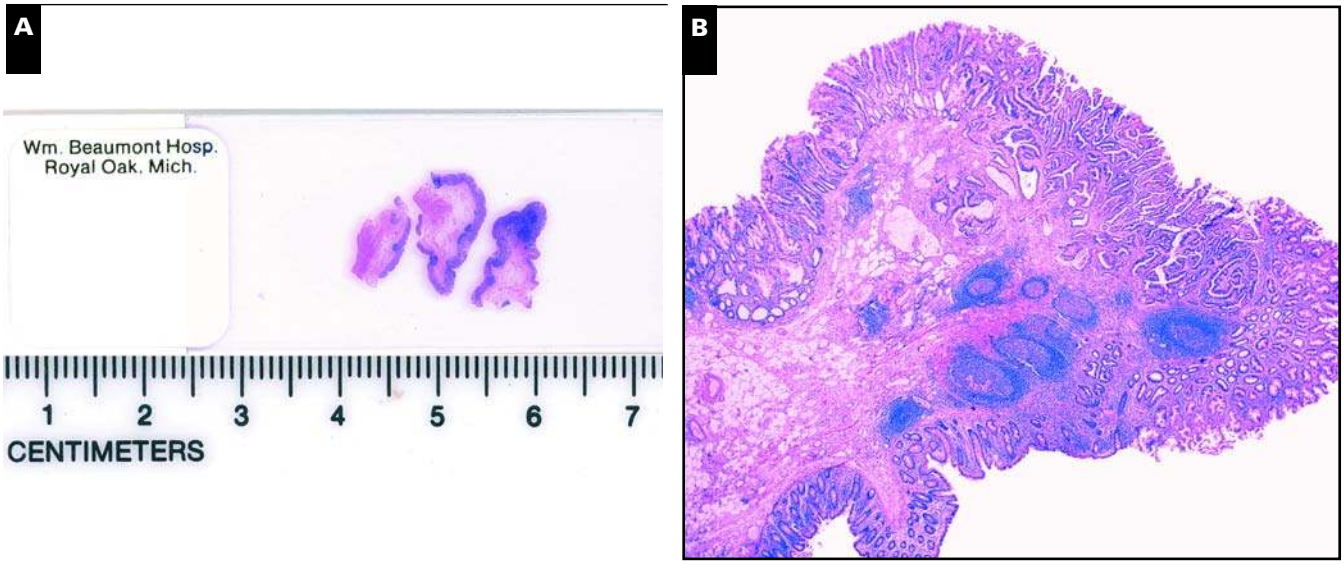

Image 19 (Case 2) Polyp slide whole-mount image (left) and microscopic panoramic low magnification overview (right, H&E, ×8).

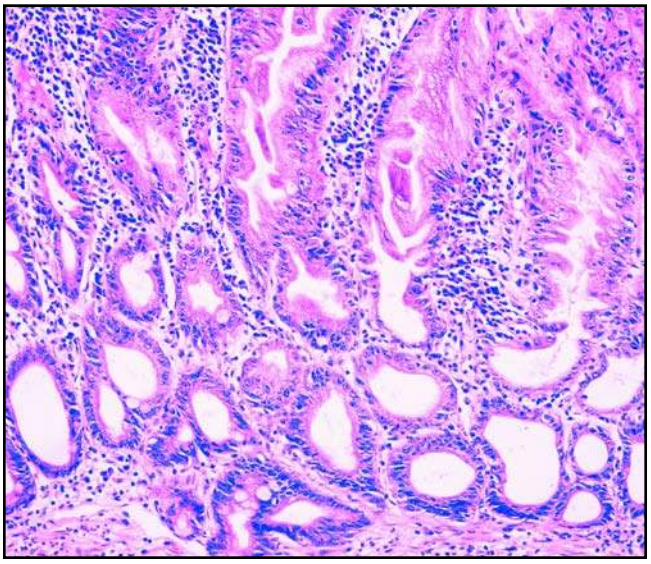

Image 20 (Case 2) Sessile serrated adenoma adjacent to invasive adenocarcinoma. The cells in the lower half of the mucosa are uniformly cuboidal with minimal cytoplasm and have oval to round nuclei with prominent nucleoli. At the mid crypt level, the cells abruptly begin to acquire abundant, lightly amphophilic cytoplasm (H&E, ×128).

dysplastic epithelial cells. No cases had high-grade APC-type dysplasia. In foci, high-grade, NOS-type dysplastic epithelial cells shared some cytologic features of high-grade, APC-type dysplasia, including large, columnar nuclei and ample eosinophilic cytoplasm; however, the NOS-type dysplastic cells in these foci were more oval, the nucleolus was more prominent, and their chromatin was less dense and coarse than in APC-type dysplasia. In the 5 cases with high-grade, serrated-type and NOS-type dysplasia, some crypts were lined by an admixture of these 2 distinct cell types, whereas other crypts were lined by cells with intermediate cytologic features.

High-grade dysplastic epithelial cells in the mid and upper crypt regions displayed maturational changes consisting of slightly smaller nuclei, more condensed chromatin, and greater amounts of amphophilic or mucinous cytoplasm compared with the subjacent, high-grade dysplastic cells in the crypt bases. Gastric foveolar mucin cell differentiation, either as columnar clear mucin or microvesicular cells, was prominent and extensive. Cells in the superficial crypt regions often were pseudostratified but otherwise had no cytologic features in common with APC-type epithelial dysplasia. Atypical, immature cells with round nuclei were present on the surface epithelium, many of which formed small tufts of cells.

Dysmaturational Crypts Adjacent to High-Grade Dysplasia

Dysmaturational crypts adjacent to high-grade epithelial dysplasia had distinctive morphologic features. In the basilar crypt regions, these crypts were lined predominantly by enteric columnar cells with admixed goblet cells. The nuclei of these cells were basilar and oval, the chromatin pattern was uniformly open, and most had small nucleoli. Within the mid crypt region, these cells displayed variable degrees of gastric foveolar mucin cell differentiation, accumulating an apical mucin pool that filled approximately half of the cell cytoplasm. The cytologic features of these cells were extremely uniform, producing a seemingly monomorphic appearance of the crypts at medium and low magnification. These dysmaturational crypts fulfilled the criteria of low-grade using the Lazarus serrated dysplasia grading system.[4]

DOI: 10.1309/V8Q9KDD5AJ9LNBAG

Table 2
Distribution of Invasive and Noninvasive Cytologic Cell Types*

	Invasive Adenocarcinoma		High-Grade Epithelial Dysplasia		
Case No.	Cuboidal-Eosinophilic	Columnar High Grade NOS	APC Type	Serrated Type	High-Grade NOS
1	30	70	0	100	0
2	30	60	0	30	70
3	20	80	0	50	50
4	10	90	0	20	80
5	40	50	0	40	50
6	30	70	0	20	80
7	—	—	0	0	100
8	—	—	0	0	100

APC, adenomatous polyposis coli; NOS, not otherwise specified.
* Data are given as percentages.

Sessile Serrated Adenomas

All 8 polyps had typical SSAs surrounding the malignant lesion. Although the architectural shapes and cytologic features of epithelial cells varied within and between polyps, the cases were unified by a similar underlying process that resulted in crypts with an expanded epithelial cell proliferation zone, delayed and decreased cell maturation, and altered or perturbations in cytoplasmic differentiation. Gastric foveolar columnar mucin cell differentiation was prominent in crypts. Cells with enteric and goblet mucus cell differentiation were admixed. Some crypt SSA cells had abundant eosinophilic cytoplasm, many of which contained small mucin vesicles.

Ancillary Studies

By study inclusion criteria, all 6 invasive adenocarcinomas and the 2 high-grade dysplasia-only cases were MSI-high and had absent hMLH1 nuclear immunoreactivity **Table 3**. Microsatellite instability could be evaluated in the high-grade dysplasia adjacent to invasive adenocarcinoma in 4 of 6 cases. In these 4 cases, the high-grade dysplasia also was MSI-high. The stutter peak pattern in the high-grade dysplasia had a pattern different from that of the corresponding invasive adenocarcinoma in all 4 cases. Of the 8 SSAs adjacent to the malignancy, 1 was MSI-low with reproducible stutter peaks in 1 microsatellite (D2s123). None of the analyzed foci of high-grade epithelial dysplasia had an LOH, single allele deletion in D5s346. β-Catenin uniformly stained the cells of high-grade dysplasia and the adjacent SSA in a membranous and cytoplasmic distribution with no or faint nuclear immunoreactivity. The intensity of membranous and cytoplasmic staining varied between crypts within each case.

Discussion

The 8 cases in this study were rare, all were endoscopically well-defined polypoid lesions, and the malignancy was a focal, early-stage process that had not yet overgrown the adjacent, nonmalignant serrated polyp. In addition, all 8 malignant neoplasms were MSI-high and had absent nuclear hMLH1 immunoreactivity, the defining molecular traits of the serrated neoplasia pathway.[12,13] Morphologically, these cases are similar to those in reports of adenocarcinoma or high-grade dysplasia arising in so-called serrated adenomas or hyperplastic polyps.[14-21] Differences between present and past cases are the larger size, greater overgrowth of the preexisting lesion by

Table 3
Ancillary Study Results in Malignant and Nonmalignant Regions

	No. of Microsatellites With Instability			Malignant Lesion Immunoreactivity	
Case No.	Invasive Adenocarcinoma	High-Grade Dysplasia	Adjacent Sessile Serrated Adenoma	Nuclear hMLH1	β-Catenin
1	5	5	0	Absent	Membrane and cytoplasm
2	5	4	0	Absent	Membrane
3	5	5	1	Absent	Membrane
4	5	5	0	Decreased to absent	Membrane
5	5	Not amplified, no result	0	Absent	Membrane and cytoplasm
6	4	Not amplified, no result	0	Absent	Membrane and cytoplasm
7	—	5	0	Absent	Membrane
8	—	4	0	Absent	Membrane and cytoplasm

DOI: 10.1309/V8Q9KDD5AJ9LNBAG

adenocarcinoma, and smaller amount of residual nonmalignant serrated lesion of most previously reported lesions. The present cases also differed from cases in previous reports in that inclusion was based on documented MSI-high status in the malignancy rather than the morphologic features of the associated serrated polyp. Conceptually, these 8 cases are smaller and earlier-stage lesions compared with the MSI-high serrated adenocarcinomas with associated serrated adenoma described by Mäkinen et al.[15]

There was a sharp transition from SSA to high-grade epithelial dysplasia and/or invasive adenocarcinoma in all 8 cases. In addition, all 6 invasive adenocarcinomas extended directly into the submucosa without lateral spread in the mucosa. The small dimension of these polyps suggests they were relatively young lesions. The size of the lesions, pattern of invasion, and lack of lateral extension is evidence that some MSI-high invasive adenocarcinomas develop rapidly and submucosal invasion occurs relatively quickly. Polyp size, calculated growth rates, and assumed intervals until neoplastic transformation for conventional tubular adenomas may not be valid models in right-colon serrated neoplasia pathway lesions. Jass[2] suggested that transformation from benign lesion to adenocarcinoma may be rapid in some serrated neoplasia pathway cases. The small size of the lesions in the present study, all of which had invaded the submucosa, is evidence that early transformation occurs when lesions are small. However, these cases offer no insight into the incidence of malignant transformation or the overall interval for the occurrence of malignant transformation. Documenting the existence of early transformation as a biologic event should not be construed as suggesting that SSAs as a group are significantly more biologically aggressive than similar-size tubular adenomas.[4] SSAs are much more common than MSI-high adenocarcinomas, suggesting they rarely progress to invasive adenocarcinoma.

Rapid transformation of a small premalignant lesion would explain the so-called interval tumor phenomenon, in which a "hyperplastic polyp" or no lesion was seen during colonoscopy 1 or 2 years preceding a large, right colon microsatellite-unstable invasive adenocarcinoma. This phenomenon often engenders bewilderment regarding how the presumed large precursor lesion could have been missed by the colleagues of the endoscopist. Although residual SSA can be found adjacent to malignancy in a minority of right colonic neoplasms,[15] small SSA polypectomy specimens containing foci of invasive adenocarcinoma or high-grade dysplasia are rare.[4] The rarity of similar cases suggests, in most cases, the premalignant component was overgrown early in the clinical life of the lesion and well before the clinical presentation.

A recent study reported 4% of right colon adenocarcinomas were endoscopically missed neoplasms.[22] Given current practice standards in North America, it is unlikely that operator error alone produced this result. Our cases provide evidence suggesting biologic factors contributed to this rate and that malignancy may not have been present at the preceding colonoscopy in all patients. The existence of small right colon premalignant lesions that undergo a temporally rapid transformation to adenocarcinoma during the interval colonoscopy also might explain why the age-adjusted incidence of right colon adenocarcinoma has remained unchanged for the past 2 decades, whereas the incidence rates of left colon and rectosigmoid adenocarcinomas have decreased substantially owing to screening colonoscopy.[23,24] This raises the question whether screening colonoscopy is less effective at identifying and removing this subset of right colon premalignant lesions before an adenocarcinoma develops.

APC-Type vs Serrated-Type Epithelial Dysplasia

The cytologic features of high-grade epithelial dysplasia in study and FAP control cases differed. In study cases, high-grade dysplastic cells were polymorphic, cuboidal to flattened columnar, with large, oval to round nuclei. Chromatin was scant, producing a clear appearance, and nucleoli were large and eosinophilic. Most cells had scant cytoplasm. Karyorrhectic debris within and around the malignant epithelium was scant. Maturational changes, including increased cytoplasm, presence of a microvesicular or an apical cytoplasmic mucin globule, decreased nuclear size, and less prominent nucleoli, were superimposed on the cytologic background features of frankly malignant cells. In contrast, high-grade dysplastic cells from patients with FAP (APC-type dysplasia) consisted of a uniform population of thin columnar cells with pencillate nuclei; coarse, hyperchromatic chromatin; relatively inconspicuous nucleoli; and abundant eosinophilic cytoplasm. The pattern and degree of nuclear shape and chromatin pattern was similar within individual adenomas and between lesions from different patients.[25] In APC-type dysplasia, no maturational changes in the superficial crypt regions were seen, and subnuclear karyorrhectic debris was abundant. Both forms of dysplasia had areas composed of undifferentiated, anaplastic, malignant cells that lacked distinctive cytologic features of either type of dysplasia. Excluding the areas in which the 2 forms of dysplasia merged into NOS-type cytologic features revealed that APC-type and serrated-type dysplasia had separate and distinctive cytologic features.

It is interesting that despite the marked cytologic dissimilarities of APC-type and serrated-type dysplasia, authors in the past have referred to both types as "adenoma."[17,26-32] Use of adenoma as a synonym for epithelial dysplasia has had a long tradition in gastrointestinal surgical pathology. As a result, all noninvasive intramucosal colonic neoplasms were conceptually and morphologically grouped as a single entity. In my opinion, students of the disease should divest themselves of this tradition. The study cases reported herein clearly demonstrate

DOI: 10.1309/V8Q9KDD5AJ9LNBAG

that not all epithelial dysplasia resembles APC-type, adenomatous dysplasia. In my opinion, *APC-type epithelial dysplasia* as a descriptive term for a set of characteristic cytologic features should be restricted to the dysplastic epithelium that comprises conventional tubular or tubulovillous adenomas. Conversely, high-grade undifferentiated epithelial dysplasia with no characteristic features of either cytologic form of dysplasia should be termed *not otherwise specified* rather than lumped together with conventional tubular adenomas. The term *serrated-type* dysplasia is a modification of the term *serrated dysplasia* used by Lazarus et al.[4]

Features of SSAs Associated With Malignant Transformation

A consistent finding in mixed hyperplastic or adenomatous and traditional serrated adenomas is the high rate of coexistent intramucosal or invasive adenocarcinoma, which supports the opinion that this group of lesions is the most advanced phase of the serrated neoplasia pathway and at high risk for malignant transformation.[26,31,33-36] In the present study cases, the crypts surrounding high-grade dysplasia had marked dysmaturational changes. These areas commonly display aberrant gastric columnar mucin cell differentiation with microvesicular, eosinophilic, or clear cytoplasm. Marked cytologic dysmaturation with highly proliferative and immature cells extending almost to the surface seems to be a key morphologic feature associated with malignant transformation.

From the Department of Anatomic Pathology, William Beaumont Hospital, Royal Oak, MI.

Address reprint requests to Dr Goldstein: Dept of Anatomic Pathology, William Beaumont Hospital, 3601 W 13 Mile Rd, Royal Oak, MI 48073.

Acknowledgment: I thank Eva Odish for her superb laboratory technical skills.

References

1. Kambara T, Simms LA, Whitehall VL, et al. *BRAF* mutation is associated with DNA methylation in serrated polyps and carcinomas of the colorectum. *Gut*. 2004;53:1137-1144.
2. Jass JR. Serrated route to colorectal cancer: back street or super highway? *J Pathol*. 2001;193:283-285.
3. Mäkinen JM, Mäkinen JM, Karttunen TJ. Serrated adenocarcinoma of the rectum associated with perianal Paget's disease: a case report. *Histopathology*. 2002;41:177-179.
4. Lazarus R, Junttila OE, Karttunen TJ, et al. The risk of metachronous neoplasia in patients with serrated adenoma. *Am J Clin Pathol*. 2005;123:349-359.
5. Hamilton SR, Vogelstein B, Kudo S, et al. Carcinoma of the colon and rectum. In: Hamilton SR, Aaltonen LA, eds. *Pathology and Genetics of Tumours of the Digestive System*. Lyon, France: IARC Press; 2000:105-119. *World Health Organization Classification of Tumours*.
6. Regitnig P, Moser R, Thalhammer M, et al. Microsatellite analysis of breast carcinoma and corresponding local recurrences. *J Pathol*. 2002;198:190-197.
7. Hao X, Frayling IM, Willcocks TC, et al. beta-Catenin expression and allelic loss at APC in sporadic colorectal carcinogenesis. *Virchows Arch*. 2002;440:362-366.
8. Umar A, Boland CR, Terdiman JP, et al. Revised Bethesda guidelines for hereditary nonpolyposis colorectal cancer (Lynch syndrome) and microsatellite instability. *J Natl Cancer Inst*. 2004;96:261-268.
9. Berg KD, Glaser CL, Thompson RE, et al. Detection of microsatellite instability by fluorescence multiplex polymerase chain reaction. *J Mol Diagn*. 2000;2:20-28.
10. Boland CR, Thibodeau SN, Hamilton SR, et al. A National Cancer Institute workshop on microsatellite instability for cancer detection and familial predisposition: development of international criteria for the determination of microsatellite instability in colorectal cancer. *Cancer Res*. 1998;58:5248-5257.
11. Oda S, Maehara Y, Ikeda Y, et al. Two modes of microsatellite instability in human cancer: differential connection of defective DNA mismatch repair to dinucleotide repeat instability. *Nucleic Acids Res*. 2005;33:1628-1636.
12. Jass JR. Hyperplastic polyps and colorectal cancer: is there a link? *Clin Gastroenterol Hepatol*. 2004;2:1-8.
13. Jass JR. Limitations of the adenoma-carcinoma sequence in colorectum. *Clin Cancer Res*. 2004;10:5969-5970.
14. Fenoglio-Preiser CM, Noffsinger AE, Stemmermann GN, et al. Carcinomas and other epithelial and neuroendocrine tumors of the large intestine. In: *Gastrointestinal Pathology: An Atlas and Text*. 2nd ed. Philadelphia, PA: Lippincott-Raven; 1999:909-1068.
15. Mäkinen JM, George SMC, Jernvall P, et al. Colorectal carcinoma associated with serrated adenoma-prevalence, histologic features, and prognosis. *J Pathol*. 2001;193:286-294.
16. Yashiro M, Kobayashi H, Kubo N, et al. Cronkhite-Canada syndrome containing colon cancer and serrated adenoma lesions. *Digestion*. 2004;69:57-62.
17. Sugimoto K, Kageoka M, Iwasaki H, et al. Adenocarcinoma arising from a hyperplastic polyp with adenomatous foci. *Endoscopy*. 1999;31:S59.
18. Tanaka M, Kusumi T, Sasaki Y, et al. Colonic intra-epithelial carcinoma occurring in a hyperplastic polyp via a serrated adenoma. *Pathol Int*. 2001;51:215-220.
19. Yao T, Nishiyama K, Oya M, et al. Multiple "serrated adenocarcinomas" of the colon with a cell lineage common to metaplastic polyp and serrated adenoma: case report of a new subtype of colonic adenocarcinoma with gastric differentiation. *J Pathol*. 2000;190:444-449.
20. Yao T, Tsutsumi S, Akaiwa Y, et al. Phenotypic expression of colorectal adenocarcinomas with reference to tumor development and biological behavior. *Jpn J Cancer Res*. 2001;92:755-761.
21. Tonooka T, Sano Y, Fujii T, et al. Adenocarcinoma in solitary large hyperplastic polyp diagnosed by magnifying colonoscope: report of a case. *Dis Colon Rectum*. 2002;45:1407-1411.
22. Bressler B, Paszat LF, Vinden C, et al. Colonoscopic miss rates for right-sided colon cancer: a population-based analysis. *Gastroenterology*. 2004;127:452-456.
23. Gupta AK, Melton LJ, Petersen GM, et al. Changing trends in the incidence, stage, survival, and screen-detection of colorectal cancer: a population-based study. *Clin Gastroenterol Hepatol*. 2005;3:150-158.

DOI: 10.1309/V8Q9KDD5AJ9LNBAG

24. Rabeneck L, Davila JA, El-Serag HB. Is there a true "shift" to the right colon in the incidence of colorectal cancer? *Am J Gastroenterol.* 2003;98:1400-1409.
25. Mulder JW, Offerhaus GJ, de Feyter EP, et al. The relationship of quantitative nuclear morphology to molecular genetic alterations in the adenoma-carcinoma sequence of the large bowel. *Am J Pathol.* 1992;141:797-804.
26. Longacre TA, Fenoglio-Preiser CM. Mixed hyperplastic adenomatous polyps/serrated adenomas: a distinct form of colorectal neoplasia. *Am J Surg Pathol.* 1990;14:524-537.
27. Batts KP. Serrated colon polyps: an update. *Pathol Case Rev.* 2004;9:173-182.
28. Jeevaratnam P, Cottier DS, Browett PJ, et al. Familial giant hyperplastic polyposis predisposing to colorectal cancer: a new hereditary bowel cancer syndrome. *J Pathol.* 1996;179:20-25.
29. Torlakovic E, Skovlund E, Snover DC, et al. Morphologic reappraisal of serrated colorectal polyps. *Am J Surg Pathol.* 2003;27:65-81.
30. Torlakovic E, Snover DC. Serrated adenomatous polyposis in humans. *Gastroenterology.* 1996;110:748-755.
31. Oh K, Redston M, Odze RD. Support for hMLH1 and MGMT silencing as a mechanism of tumorigenesis in the hyperplastic-adenoma-carcinoma (serrated) carcinogenic pathway in the colon. *Hum Pathol.* 2005;36:101-111.
32. Kuribayashi K, Ishii T, Ishidate T, et al. Two cases of inverted hyperplastic polyps of the colon and association with adenoma. *Eur J Gastroenterol Hepatol.* 2004;16:107-112.
33. Iwabuchi M, Sasano H, Hiwatashi N, et al. Serrated adenoma: a clinicopathological, DNA ploidy, and immunohistochemical study. *Anticancer Res.* 2000;20:1141-1147.
34. Jaramillo E, Watanabe M, Rubio CA, et al. Small colorectal serrated adenomas: endoscopic findings. *Endoscopy.* 1997;29:1-3.
35. Yao T, Kouzuki T, Kajiwara M, et al. "Serrated" adenoma of the colorectum, with reference to its gastric differentiation and its malignant potential. *J Pathol.* 1999;187:511-517.
36. Rubio CA, Jaramillo E. Flat serrated adenomas of the colorectal mucosa. *Jpn J Cancer Res.* 1996;87:305-309.

DOI: 10.1309/V8Q9KDD5AJ9LNBAG